



Title	Gas-Liquid Mass Transfer in Simulated Turbulent Wake Flow
Author(s)	Kumagai, Takehiko; Iguchi, Manabu; Uemura, Tomomasa; Yonehara, Noriyoshi
Citation	ISIJ International, 42(1), 112-114 <a href="https://doi.org/10.2355/isijinternational.42.112">https://doi.org/10.2355/isijinternational.42.112</a>
Issue Date	2002-01-15
Doc URL	<a href="http://hdl.handle.net/2115/75025">http://hdl.handle.net/2115/75025</a>
Rights	著作権は日本鉄鋼協会にある
Type	article
File Information	16-T. Kumagai-4.01.pdf



[Instructions for use](#)

**Note**

**Gas–Liquid Mass Transfer in Simulated Turbulent Wake Flow**

Takehiko KUMAGAI, Manabu IGUCHI,  
Tomomasa UEMURA<sup>1)</sup> and Noriyoshi YONEHARA<sup>1)</sup>

Graduate School of Engineering, Hokkaido University, North 13,  
West 8, Kita-ku, Sapporo 060-8628 Japan.

1) Faculty of Engineering, Kansai University, 3 Chou-me, 3 Ban-  
chi, Yamate-chou, Suita-shi, Osaka-fu 564-8680 Japan.

(Received on July 26, 2001; accepted in final form on September  
29, 2001)

**1. Introduction**

In materials engineering, gas injection processes are frequently adopted to remove impurities such as oxygen and carbon.<sup>1–3)</sup> There are two types of gas dispersion patterns formed above the nozzle; bubbling and jetting. The former is realized when the gas velocity at the nozzle exit,  $v_n$ , is lower than the speed of sound,  $c$ , while the latter is realized for  $v_n \geq c$  and a gas column is formed on the nozzle. This column disintegrates into many bubbles with different diameters above a certain distance from the nozzle exit. Many bubbles are therefore generated in the molten metal bath regardless of the bubbling and jetting. The removal of impurities is closely associated with the dissolving rate of the gas into the bath. However, under such a highly turbulent condition it is difficult to evaluate the mass transfer coefficient between the bubbles and molten metal because the precise evaluation of the interfacial area is actually impossible.<sup>4–6)</sup>

As the gas flow rate increases, mass transfer at the gas–liquid interface increases. However, it is not clear whether the mass flux at the gas–liquid interface is attributed to the enhancement of the interfacial area  $A$  or to the enhancement of the mass transfer coefficient  $k$ . Accordingly, previous researchers<sup>7–13)</sup> introduced the volumetric mass transfer coefficient defined as  $kA/V$ , where  $V$  is the bath volume.

In a series of studies<sup>14–18)</sup> on gas injection, the authors have tried to elucidate the contributions of the interfacial area and the mass transfer coefficient to the volumetric mass transfer coefficient. The mass transfer coefficient at a gas–liquid interface exposed to two types of liquid jets shown in Figs. 1(a) and 1(b) were measured.<sup>18)</sup> CO<sub>2</sub> gas was supplied with a syringe into a top lance to form a gas–liquid interface at the exit of the top lance. Accordingly, the gas–liquid interfacial area can be measured with sufficient accuracy. The flow fields around the gas–liquid interface thus exposed to the two types of jets are models for the flow fields around the top and side of a bubble rising in a highly turbulent flow field. In this study the gas–liquid interface was exposed to a turbulent wake flow, as shown in Fig. 1(c). This study therefore is intended to clarify the mass transfer coefficient at the rear part of a bubble.

**2. Experimental Apparatus and Procedure**

Figure 2 shows a schematic of the experimental apparatus. Distilled water was circulated with a pump. The water flow rate was controlled with a flow control valve. A top lance made of a glass pipe was enclosed with a transparent glass pipe with a larger diameter. The water passed between the two pipes. Glass wool was used as a flow straightner. CO<sub>2</sub> gas was supplied with a syringe so that a gas–liquid interface was formed at the lance exit.

As time elapses, the CO<sub>2</sub> gas dissolves into the water, and, as a result, the interface rises upward if the CO<sub>2</sub> gas is not fed. The CO<sub>2</sub> gas was therefore supplied continuously to keep the gas–liquid interface at the lance exit anytime. The gas–liquid interfacial area is controlled by changing the inner pipe diameter. Three pipes of different diameters were prepared. The inner cross-sectional areas are  $2.508 \times 10^{-4} \text{ m}^2$ ,  $0.498 \times 10^{-4} \text{ m}^2$  and  $0.249 \times 10^{-4} \text{ m}^2$ .

The velocity of water flow at the exit plane of the top lance was measured with a two-channel laser Doppler velocimeter. The mass transfer coefficient  $k$  was calculated from the relation<sup>19–21)</sup>:

$$m = k \cdot \Delta C \cdot (t \cdot A) \dots\dots\dots(1)$$

where  $m$  is the dissolved mass of CO<sub>2</sub>,  $\Delta C$  is the concentration difference,  $t$  is time and  $A$  is the gas–liquid interfacial area. The mass flux was determined by measuring the volume of the supplied CO<sub>2</sub> gas.

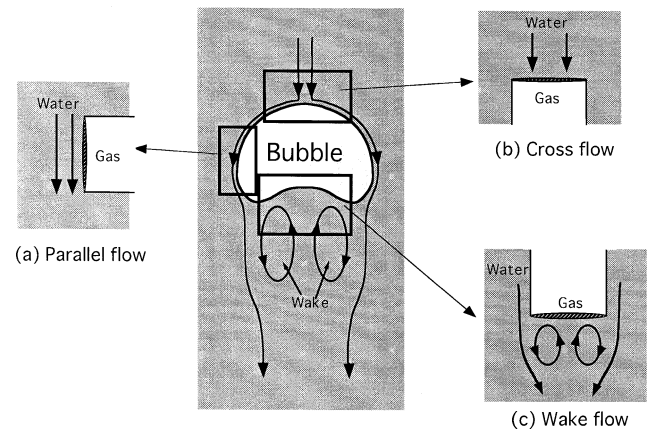


Fig. 1. Three flow models around rising bubble.

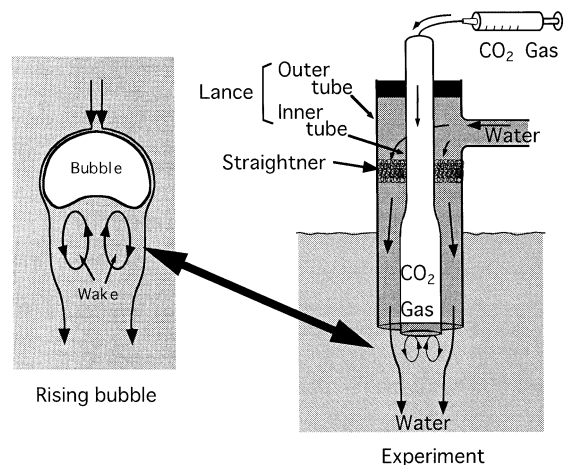


Fig. 2. Detail of top lance.

**3. Experimental Results and Discussion**

**3.1. Brief Summary of Previous Experimental Results of Mass Transfer Coefficient**

According to the previous study of the present authors,<sup>18)</sup> the mass transfer coefficient in the flow systems which are shown in Figs. 1(a) and 1(b) can be correlated in terms of the Sherwood number similitude.

$$Sh=0.664Sc^{1/3}Re^{0.5+0.1Tu} \dots\dots\dots(2)$$

$$Sh=kd/D \dots\dots\dots(3)$$

$$Re=\bar{u}d/\nu \dots\dots\dots(4)$$

$$Sc=\nu/D \dots\dots\dots(5)$$

$$Tu=u'_{rms}/\bar{u} \dots\dots\dots(6)$$

where Re is the Reynolds number, Sc is the Schmidt number,  $\bar{u}$  is the mean flow velocity,  $\nu$  is the kinematic viscosity of liquid,  $d$  is the lance diameter, and  $D$  is the diffusion coefficient,  $Tu$  is the turbulence intensity of the parallel and cross flows and  $u'_{rms}$  is the root-mean-square value of the turbulence component. The measured values of the mass flux were approximated by Eq. (2) within a scatter of  $\pm 30\%$ .

It is interesting to note that Eq. (2) approaches an empirical relation for the mass transfer coefficient at a liquid–solid interface as the Reynolds number increases,<sup>18)</sup> although the evidence is not shown here. This fact means that

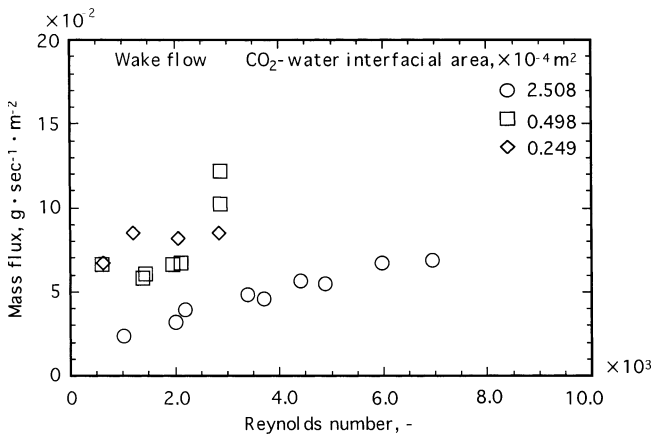


**Fig. 3.** Mass flux as a function of Reynolds number.

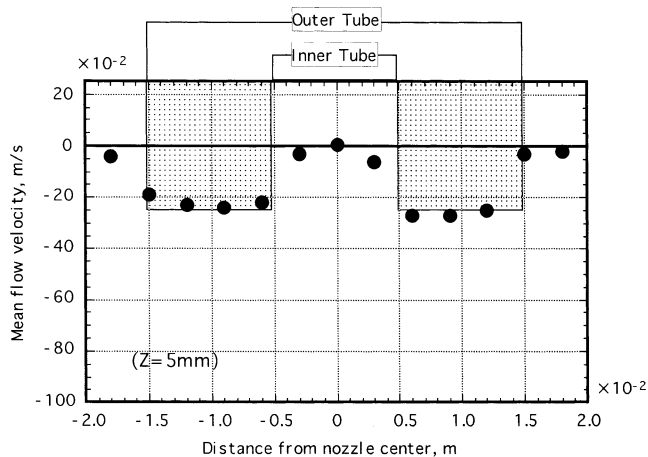


**Fig. 4.** Mean flow velocity at lance exit.

the water is fully contaminated during the measurement, and, hence, the gas–liquid interface is dirty. Considering these circumstances, experiments were carried out also in this study after much time had passed from the start of water circulation. Whether the water is contaminated or not can be judged by measuring the rising velocity of a single bubble in a still water bath.<sup>22)</sup>

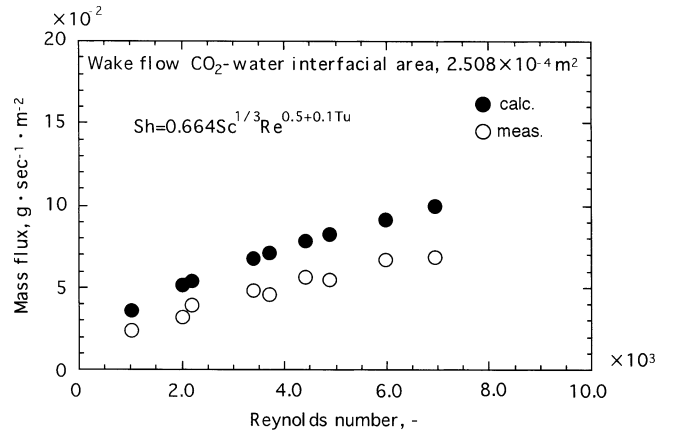
**3.2. Correlation of Mass Transfer Coefficient**

Figure 3 shows the relationship between the mass flux and the Reynolds number Re. The gas–liquid interfacial area is used as a parameter. The mass flux increased with an increase in the Reynolds number but decreased with an increase in the interfacial area. The mean velocity around the gas–liquid interface is shown in Fig. 4. The radial distribution of the mean water velocity is nearly uniform outside the gas–liquid interface. The turbulence intensity was 0.26.

The data on the mass flux for  $A=2.508 \times 10^{-4} \text{ m}^2$  are replotted in Fig. 5 together with the calculated values from Eq. (2). The measured values are smaller than the calculated values at every Reynolds number, Therefore, the coefficient in Eq. (2), 0.664, was replaced by 0.500.

$$Sh=0.500Sc^{1/3}Re^{0.5+0.1Tu} \dots\dots\dots(7)$$

All the measured values of the mass flux obtained in this



**Fig. 5.** Comparison of mass flux estimated from Eq. (2) with experimental data.

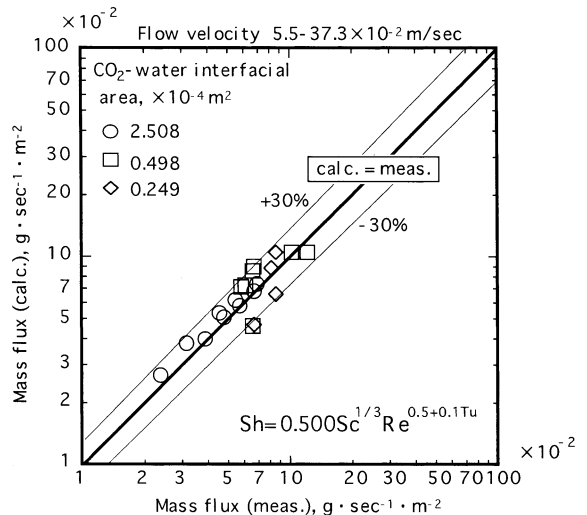


**Fig. 6.** Comparison of mass flux estimated from Eq. (7) with present experimental data.

study are compared with the calculated values from Eq. (7) in Fig. 6. The measured values can be predicted by Eq. (7) within a scatter of  $\pm 30\%$ .

#### 4. Conclusions

Model experiments were carried out to determine the mass transfer coefficient at the rear part of a bubble rising in a highly turbulent water flow. The gas-liquid interface was contaminated by surfactant.<sup>18,22)</sup> The mass transfer coefficient was nearly approximated by the empirical relation proposed in this study, Eq. (7).

#### Nomenclature

- $A$ : Gas-liquid interfacial area ( $\text{m}^2$ )  
 $c$ : Speed of sound (m/s)  
 $\Delta C$ : Concentration difference ( $\text{g}/\text{m}^3$ )  
 $D$ : Diffusion coefficient ( $\text{m}^2/\text{s}$ )  
 $d$ : Lance diameter (m)  
 $k$ : Mass transfer coefficient (m/s)  
 $m$ : Dissolved mass of  $\text{CO}_2$  gas (g)  
 $Sh$ : Sherwood number (-)  
 $Re$ : Reynolds number (-)  
 $Sc$ : Schmidt number (-)  
 $t$ : Time (s)  
 $Tu$ : Turbulence intensity (-)  
 $u$ : Mean flow velocity (m/s)  
 $u'_{\text{rms}}$ : Root-mean-square value of turbulence component (m/s)  
 $v_n$ : Gas velocity at nozzle exit (m/s)  
 $\nu$ : Kinematic viscosity of liquid ( $\text{m}^2/\text{s}$ )

#### REFERENCES

- 1) S. Inada and T. Watanabe: *Tetsu-to-Hagané*, **62** (1976), 807.
- 2) S. Inada and T. Watanabe: *Tetsu-to-Hagané*, **63** (1977), 37.
- 3) M. Kawakami, S. Dowaki, K. Hiroe and K. Itou: *Tetsu-to-Hagané*, **78** (1992), 745.
- 4) J. A. Redfield and G. Houghton: *Chem. Eng. Sci.*, **20** (1965), 131.
- 5) D. L. Wise and G. Houghton: *Chem. Eng. Sci.*, **21** (1966), 999.
- 6) H. Takemura, A. Ryu, A. Yabe and K. Konya: *Jpn. Soc. Mech. Eng.*, **62** (1996), 1467.
- 7) M. H. I. Baird and J. F. Davidson: *Chem. Eng. Sci.*, **17** (1962), 87.
- 8) J. H. Leonard and G. Houghton: *Chem. Eng. Sci.*, **18** (1963), 133.
- 9) P. H. Calderbank and A. C. Lochiel: *Chem. Eng. Sci.*, **19** (1964), 485.
- 10) A. I. Johnson, F. Besic and A. E. Hamielec: *Can. J. Chem. Eng.*, **47** (1969), 559.
- 11) P. H. Calderbank, D. S. L. Johnson and J. Loudon: *Chem. Eng. Sci.*, **25** (1970), 235.
- 12) H. Takemura and A. Yabe: *Jpn. Soc. Mech. Eng.*, (B), **64** (1998), 447.
- 13) H. Takemura and A. Yabe: *Jpn. Soc. Mech. Eng.*, (B), **64** (1998), 2168.
- 14) M. Iguchi, J. Tani, T. Uemura, H. Takeuchi and H. Kawabata: *Tetsu-to-Hagané*, **74** (1988), 1785.
- 15) M. Iguchi, J. Tani and T. Uemura: *Tetsu-to-Hagané*, **74** (1988), 2106.
- 16) M. Iguchi, H. Takeuchi, H. Kawabata, T. Uemura and Z. Morita: *Tetsu-to-Hagané*, **75** (1989), 2031.
- 17) M. Iguchi, Y. Tomita, K. Nakajima and Z. Morita: *Tetsu-to-Hagané*, **78** (1992), 1786.
- 18) T. Kumagai and M. Iguchi: *Tetsu-to-Hagané*, **87** (2001), 159.
- 19) Handbook of Heat Transfer, Jpn. Soc. Mech. Eng., Tokyo, (1962), 21.
- 20) D. Azbel: Two-phase Flows in Chemical Engineering, Cambridge University Press, Cambridge, (1981).
- 21) R. Clift, J. R. Grace and M. E. Weber: Bubbles, Drops and Particles, Academic Press, New York, (1978).
- 22) A. Tomiyama, I. Kataoka and T. Sakaguchi: *Trans. Jpn. Soc. Mech. Eng.*, (B), **61** (1995), 2357.